Identification of altered function alleles that affect *Bacillus subtilis* PerR metal ion selectivity

Zhen Ma[1], Jin-Won Lee[2] and John D. Helmann[1],*

[1]Department of Microbiology, Cornell University, Ithaca, NY, 14853-8101, USA and [2]Department of Life Science and Institute for Natural Sciences, Hanyang University, 17 Haengdang-dong, Seongdong-gu, Seoul 133-791, Republic of Korea

ABSTRACT

***Bacillus subtilis* PerR is a Fur family repressor that senses hydrogen peroxide by metal-catalyzed oxidation. PerR contains a structural Zn(II) ion (Site 1) and a regulatory metal binding site (Site 2) that, upon association with either Mn(II) or Fe(II), allosterically activates DNA binding. In addition, a third less conserved metal binding site (Site 3) is present near the dimer interface in several crystal structures of homologous Fur family proteins. Here, we show that PerR proteins with substitutions of putative Site 3 residues (Y92A, E114A and H128A) are functional as repressors, but are unexpectedly compromised in their ability to sense H_2O_2. Consistently, these mutants utilize Mn(II) but not Fe(II) as a co-repressor *in vivo*. Metal titrations failed to identify a third binding site in PerR, and inspection of the PerR structure suggests that these residues instead constitute a hydrogen binding network that modulates the architecture, and consequently the metal selectivity, of Site 2. PerR H128A binds DNA with high affinity, but has a significantly reduced affinity for Fe(II), and to a lesser extent for Mn(II). The ability of PerR H128A to bind Fe(II) *in vivo* and to thereby respond efficiently to H_2O_2 was restored in a *fur* mutant strain with elevated cytosolic iron concentration.**

INTRODUCTION

Bacillus subtilis PerR is a metal-dependent repressor that mediates adaptation to peroxide stress (1,2). PerR represses oxidative stress resistance genes including the major vegetative catalase KatA, alkyl hydroperoxide reductase AhpCF, a Dps-like iron storage protein MrgA, heme biosynthesis enzymes HemAXCDBL and a zinc uptake P-type ATPase ZosA (3). PerR is a zinc metalloprotein with a tightly bound, structural Zn(II) in metal binding Site 1 (PerR:Zn). Bound Zn(II) is required for protein stability and accumulation *in vivo* and can only be removed by protein denaturation (4). PerR:Zn can be activated for DNA binding by either Fe(II) or Mn(II) which binds at regulatory Site 2 (2,5). Structural studies reveal that PerR:Zn,Mn is in a closed conformation suitable for binding of cognate operator DNA with high affinity (6). In the presence of low levels of H_2O_2, PerR: Zn,Fe (but not PerR:Zn,Mn) undergoes metal-catalyzed oxidation of either His37 or His91 (Site 2 metal ion ligands) to 2-oxo-histidine (5,7). Oxidation leads to an open conformation of PerR and a loss of DNA binding ability (5–7). Derepression of peroxide stress genes in *B. subtilis* is therefore responsive to both the presence of H_2O_2 and the relative levels of Mn(II) and Fe(II) in the cytosol: growth of cells in low iron and high manganese impairs derepression and, as a consequence, cells are sensitized against H_2O_2 stress (8).

PerR belongs to the Fur family of metalloregulatory proteins. Fur family members often mediate metal ion homeostasis and different proteins can sense iron (Fur), zinc (Zur), nickel (Nur) or manganese (Mur) (9,10). Many, but not all, Fur family members are zinc metalloproteins with a structural site corresponding to PerR Site 1. As a general model, metal ions function as co-repressors and the metal–protein complex adopts a closed conformation capable of high affinity DNA binding (10). The precise location of metal ion sensing has not been well resolved in most cases, but both biochemical (5) and structural (6) studies assign this role to Site 2 in *B. subtilis* PerR. A third metal binding site (Site 3) has been visualized in the crystal structures of several Fur family members, and the corresponding amino acids are at least partially conserved in PerR. The role for Site 3 in mediating regulation has not been clearly established for Fur family members, although this was suggested to be the iron-sensing site for *P. aerguinosa* Fur (*Pa*Fur) (11). A recent study of

*To whom correspondence should be addressed. Tel: +1 607 255 6570; Fax: +1 607 255 3904; Email: jdh9@cornell.edu

The authors wish it to be known that, in their opinion, the first two authors should be regarded as joint First Authors.

H. pylori Fur (*Hp*Fur) suggests that Site 3 in *Hp*Fur can bind metal ion and this binding appears to have modest effect (~2-fold) on the DNA binding affinity, the biological relevance of which is yet to be established (12).

We here investigate the role of putative metal binding Site 3 in PerR function. Mutant PerR proteins with substitutions affecting residues in Site 3 retain repressor function, although their repressor activities appear to be slightly reduced compared to wild-type (WT) PerR. Unexpectedly, these mutations alter the metal selectivity for repression: the mutant proteins repress gene expression in response to Mn(II) but are defective in their ability to sense Fe(II) *in vivo*. Biochemical studies of a representative mutant (H128A) demonstrated a $\geq$10-fold decrease in Fe(II) binding affinity. This protein no longer responds to iron *in vivo*, but iron-mediated repression, and therefore the ability to sense H_2O_2, is restored in a *fur* mutant, which is derepressed for iron import (13,14). Binding studies and analysis of iron-mediated protein oxidation confirm that iron binds directly to Site 2, but provide no evidence for metal binding to Site 3. Inspection of the structure of PerR reveals a hydrogen bond network in the region corresponding in other structures to putative metal binding Site 3. We suggest that this structural element modulates the conformation, and therefore metal selectivity, of regulatory Site 2.

MATERIALS AND METHODS

Bacillus subtilis strains and growth conditions

Bacillus subtilis strains were constructed as previously described (4,5). Mutations were introduced by site-directed quickchange mutagenesis. Cells were grown at 37°C in Luria-Bertani (LB) media with appropriate antibiotics. Metal-limiting minimal media (MLMM) were prepared as described (4) with ultrapure 10 μM $FeCl_3$ or 10 μM $MnCl_2$ (Sigma Chemical Co.) added as indicated.

β-Galactosidase assay and western blot

Cells grown overnight in LB or MLMM containing both Fe and Mn were washed and inoculated (1:25 dilution) into corresponding fresh media and grown until $OD_{600} \sim 0.6$. Aliquots of cells were then treated with 100 μM H_2O_2 and further incubated for 30 min and harvested by centrifugation. β-Galactosidase assays were performed as reported (4). Western blots to determine the protein levels of C-terminal FLAG-tagged PerR in various strains were carried out using anti-FLAG antibody as described (5).

Analysis of histidine oxidation by MALDI-TOF mass spectrometry

Cells were grown and harvested in the same way as the cells used for β-galactosidase assay. After harvesting, cells were lysed and FLAG-tagged PerR variants were pulled down using Anti-FLAG M2 affinity gel as previously described (4,5). The resulting PerR samples were subjected to tryptic digestion and MALDI-TOF mass spectrometry analysis as reported (4,5).

Overexpression and purification of WT and H128A PerRs

pET16b plasmids carrying WT or H128A PerR between the NcoI and BamHI restriction sites were used for overexpression in *Escherichia coli* as described (5). Essentially, a single colony was inoculated into 10 ml of LB and grown overnight at 37°C. Cells were then diluted into 1 L of LB medium containing 0.5% glucose. 1 mM IPTG was added to the culture when OD_{600} reached ~0.6 and cells were harvested after 2 h of induction by centrifugation. After resuspension and sonication in buffer A [20 mM Tris, pH 8.0, 100 mM NaCl, 5% (v/v) glycerol] with 10 mM EDTA (ethylenediaminetetraacetic acid), the supernatant were loaded onto a heparin column pre-equilibrated with the same buffer. Proteins were eluted with a linear gradient of NaCl from 0.1 to 1 M and fractions containing PerR were combined and concentrated to load onto a Superdex 200 size exclusion column. The recovered PerR eluted was further purified using a Mono-Q column with a linear gradient of 0.1–1 M NaCl in buffer A containing 10 mM EDTA. Fractions containing PerR were concentrated and dialyzed extensively against buffer A to remove EDTA. The purified PerR was then aliquoted and frozen at −80°C. Both purified WT and H128A PerRs were $\geq$90% pure as visualized by SDS–PAGE stained by commassie blue. Protein concentrations were determined using an $\varepsilon_{277 \ nm} = 10\,400/M$ cm (5). Dimer formation of both WT and H128A were analyzed using a 12% native-PAGE gel (data not shown). Zinc contents were determined using a PAR (4-(2-Pyridylazo)resorcinol)-based assay to be more then 0.8 mol equiv per PerR monomer. WT and H128A PerRs were determined to be ~80% and 60% active, respectively, based on the amount of protein required to stoichiometrically bind 100 nM DNA which is well above the K_d for protein–DNA binding. The slight loss of activity is likely due to metal-catalyzed oxidation during purification which, as previously reported (4,5), is largely but not entirely prevented by inclusion of EDTA in purification buffers prior to the final dialysis step.

Fluorescence anisotropy experiments

A 6-carboxyfluorescein (6-FAM)—labeled *mrgA-peR* box DNA was used (5′-6-FAM-CTAAATTATAATAATTAT AATTTAG-3′ and the complement). Fluorescence anisotropy (FA) was measured with $\lambda_{ex} = 492$ nm and $\lambda_{em} = 520$ nm. For DNA binding experiments, PerR was titrated into 2 ml of buffer A containg 10 nM labeled DNA and 1 mM $MnCl_2$. FA was measured after each addition and plotted against active PerR dimer concentration. Dynafit was used to fit the data using a 1:1 non-dissociable dimer:DNA binding model (15). For Mn(II) and Fe(II) binding, increasing amounts of $MnCl_2$ or $FeCl_2$ were mixed with 120 μl buffer A containing 100 nM labeled DNA and 100 nM active PerR dimer anaerobically in a CO_2 atmosphere. FA measurements of each sample were performed immediately after

transferring to a quartz cuvette. The data were fit using a 1:1 binding model with Dynafit (15).

Electrophoretic mobility shift assays

A 250-bp ^{32}P-labeled *mrgA* promoter was used as previously reported (5). Different concentrations of PerR were incubated with the DNA probe in the binding buffer [20 mM Tris, pH 8.0, 5% (v/v) glycerol, 5 µg/ml salmon sperm DNA, 50 µg/ml bovine serum albumin (BSA), 50 mM KCl and 100 µM MnCl$_2$]. The mixtures were separated by 6% PAGE gel running with Tris-borate buffer containing 100 µM MnCl$_2$. The dried gels were then visualized using a phosphor imager.

RESULTS

Structural context of metal binding sites in PerR

The presence of up to three distinct metal binding sites in Fur family proteins has confounded attempts to elucidate the basis for metal sensing (9). PerR contains a Cys$_4$-Zn(II) structural site (Site 1) close to the C-terminus (Figure 1A, blue) and a regulatory site (Site 2) located between the DNA binding and the dimerization domain (Figure 1A, red). The regulatory site consists of residues derived from both the DNA binding and the dimerization domains, including His37 and His91 which are known targets of Fe(II)-mediated oxidation (Figure 1B). The physical location of the regulatory site is consistent with the potential to induce a protein conformational change upon metal binding or oxidation (5,9,10).

A third metal binding site (Site 3) has been observed in the crystal structures of *Mycobacterium tuberculosis* Zur (*Mt*Zur) (16), *Pseudomonas aeruginosa* Fur (*Pa*Fur) (11), *Vibrio cholerae* Fur (*Vc*Fur) (17) and *Streptomyces coelicolor* Nur (*Sc*Nur) (18) (Figure 1A, green). The positions of Site 3 in *Pa*Fur, *Vc*Fur and *Mt*Zur are nearly superimposable and many coordinating residues are conserved. These often include metal ligand(s) derived from a loop which also contributes metal ligands to regulatory Site 2. For example, in *Mt*Zur, H81 and H83 bind Zn(II) at Site 2 while H80 and H82 are involved in Zn(II)
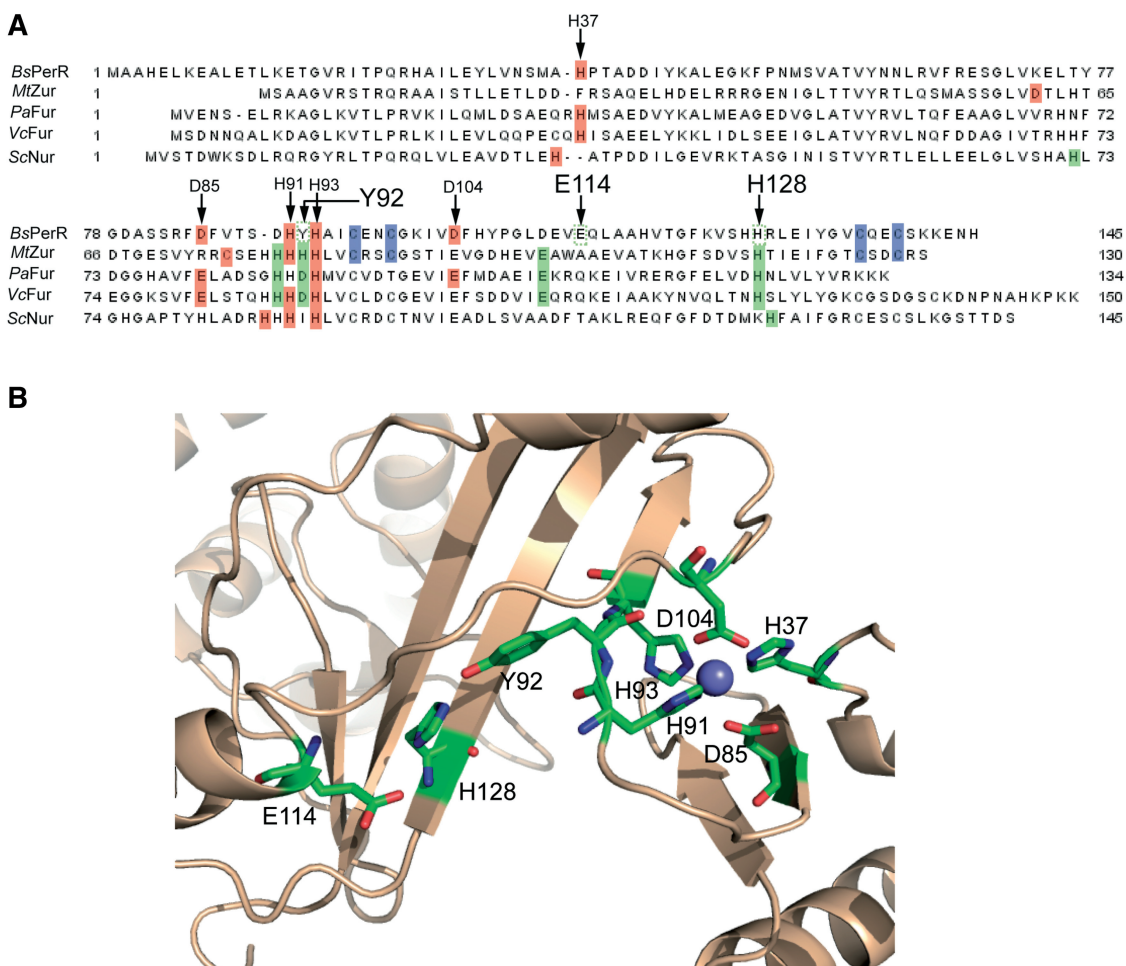

Figure 1. Metal binding sites of PerR. (**A**) Sequence alignment of *B. subtilis* PerR, *M. tuberculosis* Zur, *P. aeruginosa* Fur, *V. cholera* Fur and *S. coelicolor* Nur. Metal binding residues are highlighted based on the crystal structures: Cys$_4$-structure site (Site 1) in blue, regulatory site (Site 2) in red and Site 3 in green. Putative Site 3 residues in PerR are highlighted in dashed green boxes. Note that in *Vc*Fur and *Sc*Nur, although all four Cys residues in Site 1 are conserved, previous studies have shown that they are not functionally important (17,18) and are thus not highlighted here. (**B**) The regulatory metal binding site and Site 3 residues in the crystal structure of PerR:Zn,Mn (PDB code: 3f8n) generated using PyMOL (6).

binding at Site 3 (16). In *Pa*Fur, Site 3 was proposed to mediate iron sensing (11). Although Site 3 in *Sc*Nur only partially overlaps (Figure 1A), this site has been proposed to be the Ni(II)-sensing site (18). While the crystal structure of PerR:Zn,Mn reveals no metal bound at Site 3, sequence alignment shows that residues in Site 3 are partially conserved in PerR (Figure 1A). Therefore, we postulated that putative Site 3 of PerR (Y92, E114 and H128) (Figure 1B) might contribute to metal sensing. The identification of E114 as a candidate Site 3 residue is based on the crystal structure (6) and the observed phenotype (see below).

Mutation of putative Site 3 residues eliminates H_2O_2 responsiveness

To test the functional relevance of the putative Site 3 residues, the repressor activities of WT and PerR mutants were examined *in vivo* using a reporter fusion (P_{mrgA}-*cat-lacZ*) as described (5). β-Galactosidase activity was repressed in cells expressing WT PerR but derepressed in H37A(Site 2) or *perR* null cells (Figure 2A).

The effect of H37A is similar to previous results (5). Upon treatment with $100\,\mu M$ H_2O_2, there was a reproducible derepression of β-galactosidase activity in cells expressing WT PerR, consistent with previous results (4,5). Note that these H_2O_2 treatment conditions fully inactivate PerR as monitored by protein oxidation (5), although β-galactosidase does not accumulate to the same level as in the constitutively derepressed *perR* null strain during the 30 min treatment. All three of the PerR Site 3 mutants (H128A, Y92A and E114A) repressed the P_{mrgA}-*cat-lacZ* reporter fusion although not quite as efficiently as wild-type, ranging from 15 to 100 Miller units for the Site 3 mutants as compared to ∼5 Miller units for wild-type (Figure 2A). PerR mutants with a C-terminal FLAG-tag retain similar repressor activities to the untagged alleles (Figure 2A), and were used for protein detection and pull-down assays. The slightly reduced efficacy of the Site 3 mutants as repressors was not caused by reduced protein levels. Indeed, the mutant proteins were more abundant than WT PerR (Figure 2B). As shown previously (4,5), increased abundance is characteristic of
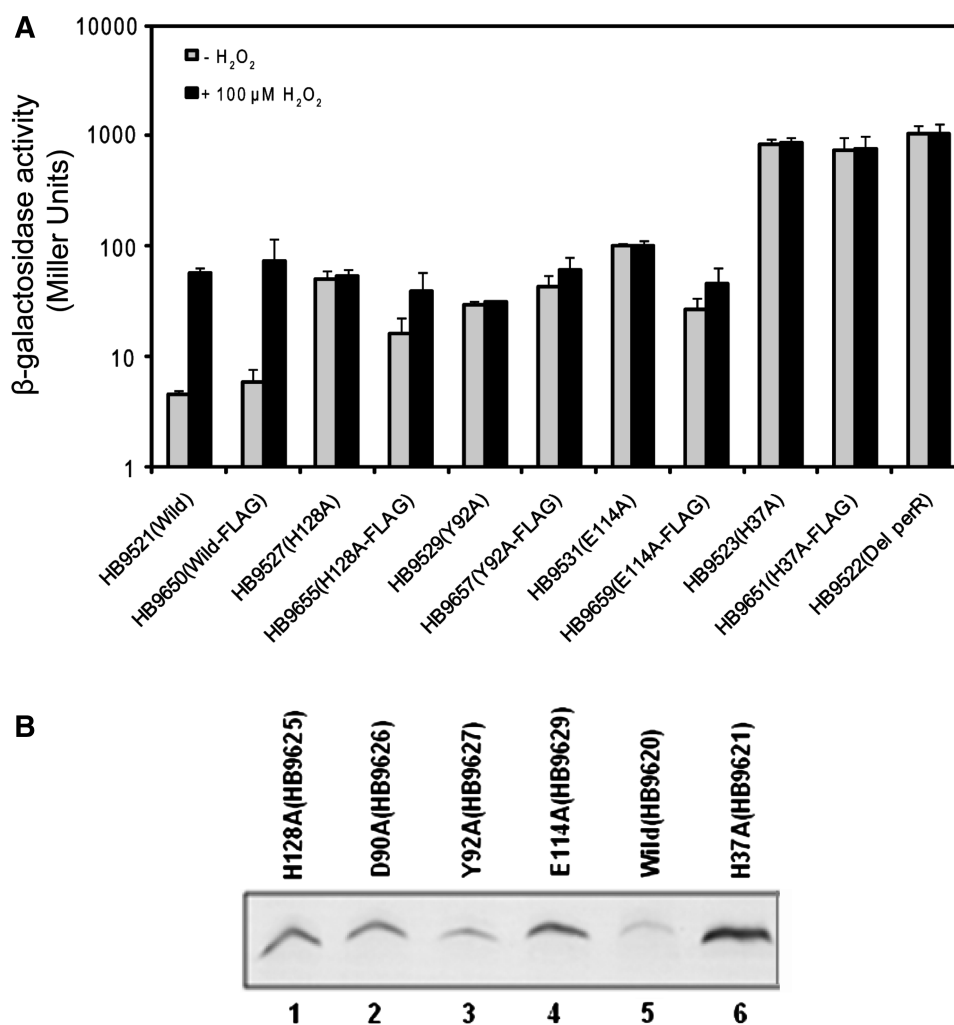

Figure 2. Repressor activities of PerR variants. (**A**) Repressor activities of PerR mutants as analyzed *in vivo* ($n = 3$) and (**B**) western blot analysis of FLAG-tagged PerR variants.

PerR proteins with reduced repressor activity since PerR is autoregulated.

Unexpectedly, the PerR Site 3 mutants were poorly or non-responsive to H_2O_2 (Figure 2A). Consistently, FLAG-tagged Site 3 mutants were slightly responsive to H_2O_2. The observed induction was consistently higher than observed for untagged Site 3 mutant alleles, but was still much less than observed for wild-type. This difference presumably reflects a minor effect of the C-terminal FLAG-tag on protein stability or conformation. Since Fe(II) but not Mn(II) binding at the regulatory site is essential for H_2O_2 induced derepression (5), this observation is consistent with the hypothesis that these Site 3 residues are involved in metal binding, either directly or indirectly. Both *in vivo* and *in vitro* experiments were therefore carried out to determine the exact role of Site 3 in PerR.

A Site 3 PerR mutant (H128A) can still bind DNA with high affinity *in vitro*

One simple explanation for the reduced repressor activities of the Site 3 mutants is that they are unable to bind the *mrgA* operator site with the same affinity as WT PerR. To test this and to assess the properties of PerR mutants *in vitro*, both WT and H128A PerR (as a representative Site 3 mutant) were overexpressed and purified from *E. coli*. Both purified proteins formed stable dimers with or without Mn(II) as monitored by native-PAGE (data not shown). Moreover, both proteins bound the *mrgA* promoter with indistinguishable high affinity (Figure 3A) as monitored by FA. In both cases, binding was saturated at ~1.0 active dimer per DNA, therefore only a lower limit of the binding affinity of 10^9/M can be deduced from these data. To obtain more quantitative measurements of DNA binding affinity, Electrophoretic mobility shift assays (EMSA) studies were conducted which revealed that both WT and H128A PerR proteins bound DNA with half occupancy detected at ~10 nM monomer ($K = 10^8$/M). In contrast, no DNA binding was detected for the Site 2 mutant H37A under these conditions (Figure 3B). The difference in the apparent DNA binding affinities obtained by these two methods may result from different solution conditions (see 'Materials and Methods' section). Nevertheless, both assays indicate that H128A and WT PerR bind DNA with comparable affinity, and therefore account for neither the slightly reduced repressor activity nor the loss of H_2O_2 responsiveness of the H128A mutant *in vivo*. Moreover, this also indicates that the allosteric switch into a high DNA binding affinity conformation upon metal binding is not affected in H128A PerR.

Site 3 mutant PerR proteins respond *in vivo* to Mn(II), but not to Fe(II)

The repressor activity of PerR is known to require a bound metal ion at Site 2 [typically either Mn(II) or Fe(II)] and the identity of the bound metal determines peroxide responsiveness (5). To determine if the Site 3 PerR mutants were altered in their metal binding properties *in vivo*, β-galactosidase assays were carried
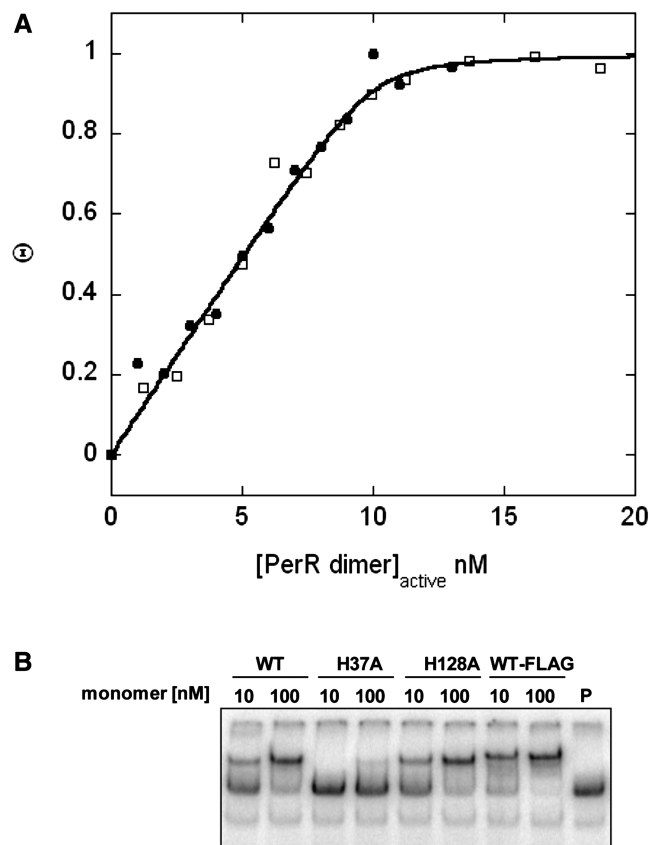
Figure 3. DNA binding of WT and H128A PerRs. (**A**) Normalized DNA binding curves of WT (filled circle) and H128A (open square) PerRs in presence of Mn(II) monitored by FA. Solid curve represents the simulated binding curve using an affinity of 10^9/M. Conditions: 10 nM DNA, 1 mM $MnCl_2$, 20 mM Tris, pH 8.0, 0.1 M NaCl, 5% (v/v) glycerol and (**B**) DNA binding of WT and H128A in presence of Mn(II) determined using EMSA. Protein concentrations are as indicated and the free DNA probe designated P is shown in the last lane.

out in cells grown in metal-limiting minimal medium (MLMM) with or without activating levels of Mn(II) or Fe (added as Fe(III)). Both WT and the Site 3 PerR variants were unable to repress β-galactosidase expression when grown in MLMM lacking added Mn or Fe, consistent with the requirement for a metal ion as co-repressor (Figure 4). As expected, addition of either Mn or Fe restored repression by WT PerR *in vivo*. Interestingly, the Site 3 mutants of PerR responded to Mn, but not to Fe. This Mn(II)-selective response is distinct from the regulatory Site 2 mutant H37A for which neither Mn nor Fe can serve as co-repressor (Figure 4). These observations are consistent with the loss of H_2O_2 responsiveness (Figure 2A), suggesting that the Site 3 mutants may indeed be defective in Fe(II) binding.

Activation of PerR by Fe(II) does not involve direct binding of Fe(II) to Site 3

The inability of Site 3 mutants to respond to Fe *in vivo* might indicate that Fe(II) is sensed by binding to this site, whereas Site 2 is necessary and sufficient for sensing Mn(II). However, previous studies have shown that
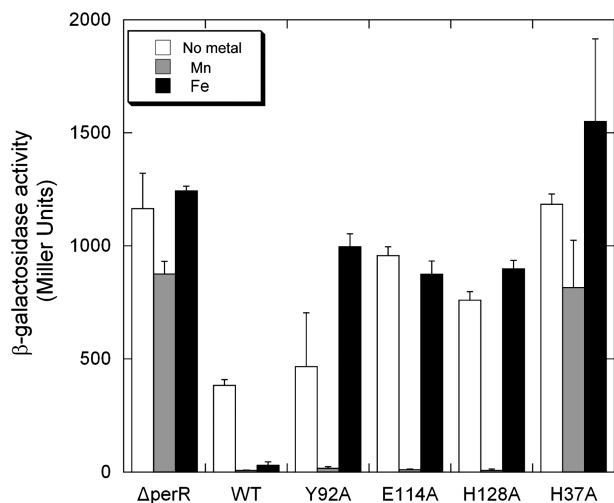
Figure 4. Metal-dependent repressor activities of PerR variants. Cells were grown in MLMM with no metal or activating concentrations (10 μM) of Mn or Fe added as indicated. β-Galactosidase assays were carried out in triplicate with cells harvested at mid-logarithmic phase.

(i) sensing of H_2O_2 requires Fe(II) and leads to oxidation of Site 2 metal ligands H37 and H91 and (ii) the binding of Fe(II) is competitive with Mn(II) (5) which has been visualized in Site 2 by X-ray crystallography and X-ray absorption spectroscopy (6). Thus, Fe(II) clearly binds at Site 2, but this does not preclude a possible second binding event at Site 3.

To test the hypothesis that the response to Fe(II) requires metal binding at both Sites 2 and 3, we monitored the stoichiometry of metal binding using an FA-based DNA binding assay (4). In this assay, increasing amounts of Fe(II) or Mn(II) were mixed anaerobically with 100 nM 6-FAM-labeled *mrgA* DNA and 100 nM active PerR dimer. Since metal-bound PerR binds DNA with high affinity ($K_a \geq 10^9$/M) under these conditions (Figure 3A), metallated PerR will bind stoichiometric amounts of DNA and the change in FA is a direct reporter of metal binding to PerR (4). Under these conditions, WT PerR binds stoichiometric amounts of Fe(II) as indicated by the linear increase and saturation at ~200 nM, or ~2.0 mol equiv. Fe(II) per active PerR dimer (Figure 5A). Importantly, this suggests that one Fe(II) per PerR subunit is sufficient to activate DNA binding. We assign the regulatory site (Site 2) as responsible for metal binding, as already visualized in the crystal structure of PerR bound to Mn(II) (5,6). We therefore suggest that the role of these Site 3 residues is instead to stabilize an active conformation of PerR. However, it remains possible that one or more residues assigned to Site 3 might re-orient to interact with Fe(II) bound at Site 2 since, at present, only the Mn(II) bound form of PerR has been visualized by high resolution structural approaches (6).

The PerR H128A mutation selectively reduces the affinity of Fe(II) for Site 2

Based on these findings, we hypothesized that the key role of Site 3 residues might be to stabilize a conformation
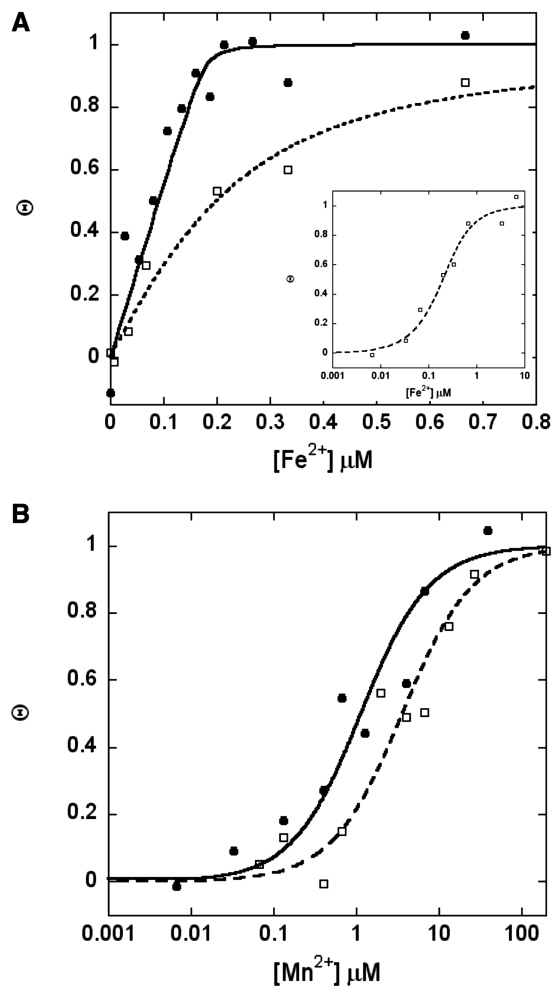

Figure 5. Fe(II) and Mn(II) binding to WT and H128A PerRs *in vitro*. Normalized binding curves indicating (**A**) Fe(II) and (**B**) Mn(II) binding to WT (filled circle, solid line) and H128A (open square, dashed line) PerRs monitored by FA. In all cases, the curves represent the best fit to a 1:1 binding model. The linear scale is used in panel (A) to show the stoichiometry of Fe(II) binding to WT PerR. The inset shows the full binding curve of Fe(II) to PerR H128A. Conditions: 100 nM DNA, 100 nM active PerR dimer, 20 mM Tris, pH 8.0, 0.1 M NaCl, 5% (v/v) glycerol.

important for the interaction of Fe(II) with the adjacent Site 2. We therefore compared the affinity of WT and H128A PerR proteins for Mn(II) and Fe(II) using this same FA assay. Under these conditions, WT PerR binds Fe(II) with an affinity $\geq 10^8$/M, whereas H128A PerR binds Fe(II) much more weakly (Figure 5A and inset). Data fitting using a simple 1:1 binding model revealed a binding affinity for H128A PerR of 1.0 (± 0.2) × 10^7/M, or $\geq$10-fold less than that of WT, consistent with its inability to use Fe(II) as a co-repressor *in vivo* (Figure 4). For Mn(II), the binding affinities were closer, with association constants of 9.5 (± 2.3) × 10^5/M for WT and 2.8 (± 0.6) × 10^5/M for H128A. Although H128A PerR binds Mn(II) somewhat less tightly than WT, this affinity is clearly sufficient to mediate Mn(II) responsiveness *in vivo* (Figure 4), where intracellular free Mn(II) levels are determined by the affinity of the manganese

homeostasis regulator MntR for Mn(II) (19–21). We conclude that mutations in the Site 3 residue H128A affect the conformation of Site 2 and selectively impair the productive interaction of Fe(II) with this site.

Sensing of Fe(II), and peroxide responsiveness, is restored to PerR Site 3 variants in a *fur* mutant background

We reasoned that if Site 3 mutants were affecting the binding of Fe(II) to Site 2, it might be possible to overcome the reduced binding affinity by elevating the levels of iron in the cell. The bioavailable pool of Fe is regulated by Fur and *fur* mutants have an elevated level of cell-associated iron (20). As predicted, these Site 3 mutants efficiently utilize Fe as a co-repressor in a *fur* mutant background when grown in MLMM (data not shown). To demonstrate that this was due to a restoration of Fe(II) binding at Site 2, we monitored the ability of PerR and Site 3 mutants to respond to H_2O_2 in the *fur* mutant background. Indeed, in this background the FLAG-tagged PerR Site 3 mutants responded as well as wild-type to added H_2O_2 (Figure 6A). Note that the low level H_2O_2 responsiveness of these mutants, as observed in WT cells, is consistent with the results for C-terminal FLAG-tagged proteins as noted in Figure 2A. To demonstrate that H_2O_2 responsiveness is due to Fe(II) occupancy of Site 2 *in vivo*, we monitored the Fe(II)-mediated site-specific protein oxidation of Site 2 resides H37 and H91 by MALDI-TOF spectrometry (5). Consistent with our predictions, FLAG-tagged H128A PerR from WT cells treated with H_2O_2 was not significantly oxidized (Figure 6C, top), whereas H128A protein recovered from H_2O_2-treated *fur* mutant cells was oxidized on H37 and H91 (Figure 6C, bottom) to the same extent as WT PerR (Figure 6B). The same profile was obtained when a Site 3 double mutant, E114A/H128A, was analyzed (Figure 6D). These oxidation patterns are consistent with the H_2O_2 responsiveness observed by β-galactosidase assays (Figure 6A). Collectively, these studies indicate that PerR Site 3 variants can be readily metallated by Mn(II), but not by Fe(II), in wild-type cells while the increased intracellular Fe in *fur* cells now enables these variants to bind Fe(II). These results support the hypothesis that Site 3 residues are not themselves required for Fe(II) binding, but that this region of PerR may affect the conformation, and therefore binding affinity, of Site 2 for Fe(II).

DISCUSSION

The conservation of metal binding Site 3 among many Fur family proteins suggests its functional importance, an inference supported by previous mutational analyses (18,22) and those of this study. However, whether the role of 'Site 3' residues involves direct metal binding, or some other role in protein structure, is unclear. The major evidence supportive of the direct binding of divalent metal ions at Site 3 is from structural analyses of proteins, which were sometimes grown with very high levels of metal ions [e.g. 10 mM Zn^{2+} for *Pa*Fur (11); 0.1 mM $NiCl_2$ for
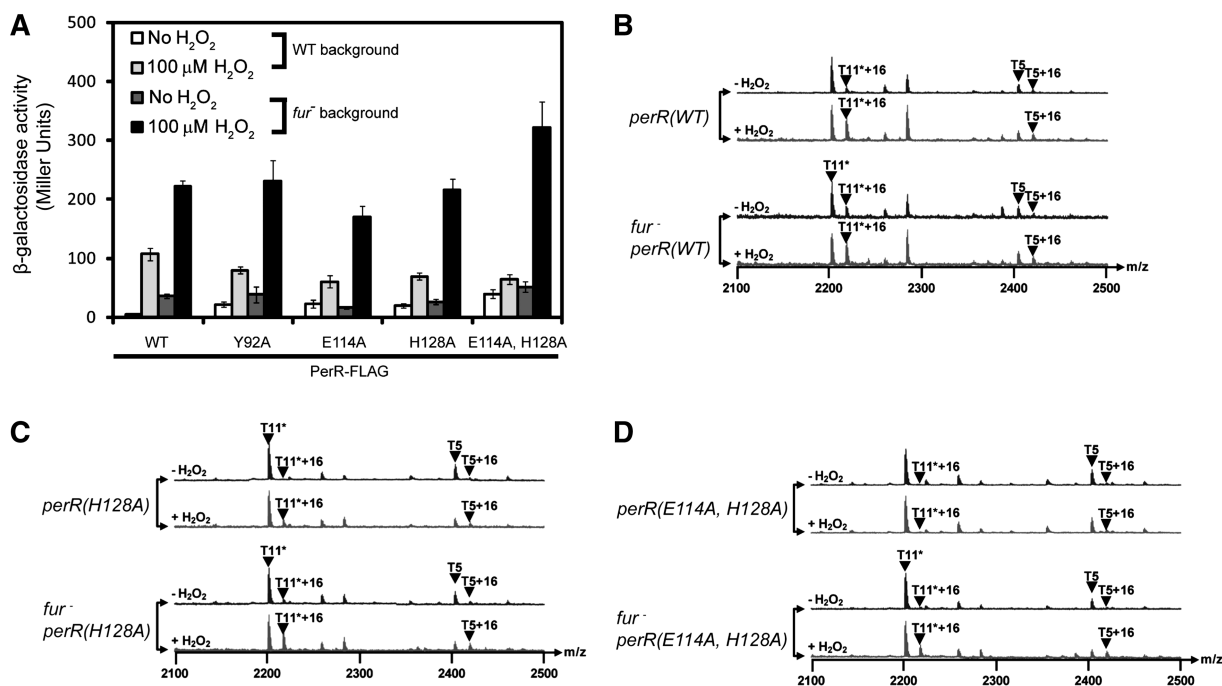

Figure 6. Functional analysis of Site 3 PerR variants in *fur* cells. (**A**) Repressor activities of FLAG-tagged PerR Site 3 variants with or without H_2O_2 treatment in WT and *fur* cells grown in LB medium as indicated. (**B–D**) MALDI-TOF spectrometry of tryptic digested FLAG-tagged PerR (B) WT, (C) H128A and (D) E114A/H128A pulled down from WT (top) and *fur* (bottom) cells with or without H_2O_2 treatment as indicated. In all experiments, *B. subtilis* strains (*perR::tet, amyE::perR-FLAG*) were used with or without incorporation of *fur::kan*. PerR variants were expressed from the *amyE* locus. Expected molecular weights for the tryptic peptides containing H37 (T5: H25 to K45) and H91 (T11*: F84 to K101 with carbamidomethyl-modified Cys96 and Cys99 as a result of iodoacetamide treatment) are 2401.19 and 2199.93, respectively. Peaks designated as T5+16 and T11*+16 represent the corresponding oxidation products (5).

*Sc*Nur (18)]. Moreover, extant crystal structures reveal significant differences among Fur family proteins. For instance, no metal is found at Site 3 of PerR (6); in *Mt*Zur, the corresponding Site 3 is bound with a Zn(II) ion but with only ~50% occupancy and the protein appear to be in an inactive conformation (16); in *Pa*Fur and *Vc*Fur, there are metals bound at Site 3 and both proteins are in the active form (11,17); in *Sc*Nur, the corresponding Site 3 consists of residues different from PerR (Figure 1A) and is proposed to be the Ni(II)-sensing site (18). Whether or not the observed metal binding events occur with a physiologically relevant affinity has not been determined and Site 3 may indeed play different roles in different proteins. Due to its location near the dimer interface, Site 3 may stabilize protein structure or facilitate dimerization, may be involved in direct metal binding and sensing, or may communicate regulatory site occupancy with the rest of the molecule.

PerR binds either Mn(II) or Fe(II) in regulatory Site 2 and both metals adopt the same penta-coordinate, square pyramidal geometry. However, only the Fe(II)-bound form (PerR:Zn,Fe) responds to physiological levels of peroxides (5,6). Our results indicate that one Fe(II) per PerR subunit is sufficient to activate DNA binding, which along with previous biochemical and structural studies, suggests the putative Site 3 is not directly involved in metal binding. However, the residues in the putative Site 3 binding pocket do appear to affect the metal binding affinity of regulatory Site 2 and thereby the metal specificity of PerR *in vivo*.

Inspection of the PerR structure leads us to suggest that these three 'Site 3' residues form a hydrogen bonding network at the dimer interface that is important for determining the precise coordination geometry, and hence metal selectivity, of regulatory Site 2. Remarkably, mutations in this region (putative Site 3 residues Y92A, E114A and H128A) all have similar effects on metal responsiveness (Figure 4). This suggests that these three residues are functionally linked. Both Y92 and E114 are in hydrogen bonding distances to H128, with 2.42 Å between the Y92 hydroxyl oxygen and Nε2 of H128, 2.57 Å between Nδ1 of H128 and E114 carboxyl oxygen (Figure 1B) based on the crystal structure (6). Moreover, regulatory and Site 3 residues are interdigitated along the primary sequence of PerR with Site 3 residue Y92 between two Site 2 ligands, His91 and His93 (Figure 1). Thus, Y92 hydrogen bonding may affect local conformation and dynamics of this loop region, thereby modulating metal binding geometry and affinity at Site 2. Since Fe(II) binding by H128A PerR is more significantly affected than Mn(II) binding, as supported by both *in vitro* and *in vivo* studies presented here, we suggest that the Fe(II) may be more sensitive than Mn(II) to the precise protein conformation in this region. In general, this region of Fur proteins is His-rich and often includes residues in a loop with alternating orientation toward sites 2 and 3 (Figure 1A). Such an organization may allow some conformational flexibility (e.g. ligand recruitment), which is one complication when interpreting mutagenesis results for the Fur family proteins.

Hydrogen bonding networks around metal sensing sites, either with or without the direct involvement of metal coordinating residues, are also important for the function of other metalloregulators. For example, hydrogen bonds between the high affinity Ni(II) binding sites in NikR tetramer are proposed to be important for high affinity Ni(II) binding (23). In other cases, hydrogen bonds in CsoR and CzrA involving key metal binding ligands are known to modulate allosteric regulation (10,24).

This study also presents an intriguing example where the bioavailability of metal ions determines the metal specificity *in vivo*. Coordination geometry, another major metal specificity determinant, is insufficient because both Mn(II) and Fe(II) can be well fit into the five-coordinate square pyramidal environment in PerR, as shown by both crystallography and X-ray absorption spectroscopy (6). The findings here suggest that Site 3 residues in PerR modulate the binding affinity and in concert with regulatory circuits controlling bioavailable metal concentrations determines *in vivo* metal specificity. Such observations share interesting parallels with previous results on the metal specificity of *Corynebacterium diphtheriae* DtxR when it was expressed in *B. subtilis* (13). While the total concentrations of different metal ions in the cell are relatively easy to measure by methods such as ICP-MS, the bioavailable concentrations of metal ions are difficult to measure directly and are usually inferred from metal affinities of those metalloregulatory proteins controlling uptake and efflux (25). Understanding intracellular metal speciation, and its effects on the regulatory circuitry, remains as a major challenge in understanding cellular metal ion homeostasis.

FUNDING

Conflict of interest statement. None declared.

REFERENCES

1. Bsat,N., Herbig,A., Casillas-Martinez,L., Setlow,P. and Helmann,J.D. (1998) *Bacillus subtilis* contains multiple Fur homologues: identification of the iron uptake (Fur) and peroxide regulon (PerR) repressors. *Mol. Microbiol.*, **29**, 189–198.
2. Herbig,A.F. and Helmann,J.D. (2001) Roles of metal ions and hydrogen peroxide in modulating the interaction of the *Bacillus subtilis* PerR peroxide regulon repressor with operator DNA. *Mol. Microbiol.*, **41**, 849–859.
3. Helmann,J.D., Wu,M.F., Gaballa,A., Kobel,P.A., Morshedi,M.M., Fawcett,P. and Paddon,C. (2003) The global transcriptional response of *Bacillus subtilis* to peroxide stress is coordinated by three transcription factors. *J. Bacteriol.*, **185**, 243–253.
4. Lee,J.W. and Helmann,J.D. (2006) Biochemical characterization of the structural Zn^{2+} site in the *Bacillus subtilis* peroxide sensor PerR. *J. Biol. Chem.*, **281**, 23567–23578.
5. Lee,J.W. and Helmann,J.D. (2006) The PerR transcription factor senses H_2O_2 by metal-catalysed histidine oxidation. *Nature*, **440**, 363–367.
6. Jacquamet,L., Traoré,D., Ferrer,J.-L., Proux,O., Testemale,D., Hazemann,J.-L., Nazarenko,E., El Ghazouni,A., Caux-Thang,C.,

Duarte,V. *et al*. (2009) Structural characetrization of the active form of PerR: Insights into the metal-induced activation of PerR and Fur proteins for DNA binding. *Mol. Microbiol.*, **72**, 20–31.

7. Traore,D.A.K., Ghazouani,A.E., Jacquamet,L., Borel,F., Ferrer,J.-L., Lascoux,D., Ravanat,J.-L., Jaquinod,M., Blondin,G., Caux-Thang,C. *et al.* (2009) Structural and functional characterization of 2-oxo-histidine in oxidized PerR protein. *Nat. Chem. Biol.*, **5**, 53–59.

8. Chen,L., Keramati,L. and Helmann,J.D. (1995) Coordinate regulation of *Bacillus subtilis* peroxide stress genes by hydrogen peroxide and metal ions. *Proc. Natl Acad. Sci. USA*, **92**, 8190–8194.

9. Lee,J.W. and Helmann,J.D. (2007) Functional specialization within the Fur family of metalloregulators. *BioMetals*, **20**, 485–499.

10. Ma,Z., Jacobsen,F.E. and Giedroc,D.P. (2009) Coordination chemistry of bacterial metal transport and sensing. *Chem. Rev.*, **109**, 4644–4681.

11. Pohl,E., Haller,J.C., Mijovilovich,A., Meyer-Klaucke,W., Garman,E. and Vasil,M.L. (2003) Architecture of a protein central to iron homeostasis: crystal structure and spectroscopic analysis of the ferric uptake regulator. *Mol. Microbiol.*, **47**, 903–915.

12. Dian,C., Vitale,S., Lenoard,G.A., Bahlawane,C., Fauquant,C., Leduc,D., Muller,C., De Reuse,H., Michaud-Soret,I. and Terradot,L. (2010) The structure of the *Helicobacter pylori* ferric uptake regulator Fur reveals three functional metal binding sites. *Mol. Microbiol.* (In press).

13. Guedon,E. and Helmann,J.D. (2003) Origins of metal ion selectivity in the DtxR/MntR family of metalloregulators. *Mol. Microbiol.*, **48**, 495–506.

14. Ollinger,J., Song,K.B., Antelmann,H., Hecker,M. and Helmann,J.D. (2006) Role of the Fur regulon in iron transport in *Bacillus subtilis*. *J. Bacteriol.*, **188**, 3664–3673.

15. Kuzmic,P. (1996) Program DYNAFIT for the analysis of enzyme kinetic data: application to HIV proteinase. *Anal. Biochem.*, **237**, 260–273.

16. Lucarelli,D., Russo,S., Garman,E., Milano,A., Meyer-Klaucke,W. and Pohl,E. (2007) Crystal structure and function of the zinc uptake regulator FurB from *Mycobacterium tuberculosis*. *J. Biol. Chem.*, **282**, 9914–9922.

17. Sheikh,M.A. and Taylor,G.L. (2009) Crystal structure of the *Vibrio cholerae* ferric uptake regulator (Fur) reveals insights into metal co-ordination. *Mol. Microbiol.*, **72**, 1208–1220.

18. An,Y.J., Ahn,B.E., Han,A.R., Kim,H.M., Chung,K.M., Shin,J.H., Cho,Y.B., Roe,J.H. and Cha,S.S. (2009) Structural basis for the specialization of Nur, a nickel-specific Fur homolog, in metal sensing and DNA recognition. *Nucleic Acids Res.*, **37**, 3442–3451.

19. Que,Q. and Helmann,J.D. (2000) Manganese homeostasis in *Bacillus subtilis* is regulated by MntR, a bifunctional regulator related to the diphtheria toxin repressor family of proteins. *Mol. Microbiol.*, **35**, 1454–1468.

20. Guedon,E., Moore,C.M., Que,Q., Wang,T., Ye,R.W. and Helmann,J.D. (2003) The global transcriptional response of *Bacillus subtilis* to manganese involves the MntR, Fur, TnrA and σ^B regulons. *Mol. Microbiol.*, **49**, 1477–1491.

21. Kliegman,J.I., Griner,S.L., Helmann,J.D., Brennan,R.G. and Glasfeld,A. (2006) Structural basis for the metal-selective activation of the manganese transport regulator of *Bacillus subtilis*. *Biochemistry*, **45**, 3493–3505.

22. Bsat,N. and Helmann,J.D. (1999) Interaction of *Bacillus subtilis* Fur (Ferric Uptake Repressor) with the *dhb* Operator *In Vitro* and *In Vivo*. *J. Bacteriol.*, **181**, 4299–4307.

23. Schreiter,E.R., Sintchak,M.D., Guo,Y., Chivers,P.T., Sauer,R.T. and Drennan,C.L. (2003) Crystal structure of the nickel-responsive transcription factor NikR. *Nat. Struct. Biol.*, **10**, 794–799.

24. Eicken,C., Pennella,M.A., Chen,X., Koshlap,K.M., VanZile,M.L., Sacchettini,J.C. and Giedroc,D.P. (2003) A metal-ligand-mediated intersubunit allosteric switch in related SmtB/ArsR zinc sensor proteins. *J. Mol. Biol.*, **333**, 683–695.

25. Outten,C.E. and O'Halloran,T.V. (2001) Femtomolar sensitivity of metalloregulatory proteins controlling zinc homeostasis. *Science*, **292**, 2488–2492.